Interpolated Finite Impulse Response Filters

YRJÖ NEUVO, SENIOR MEMBER, IEEE, DONG CHENG-YU, AND SANJIT K. MITRA, FELLOW, IEEE

Abstract—**A new approach to implement computationally efficient finite impulse response (FIR) digital filters is presented. The filter structure is a cascade of two sections. The first section generates a sparse set of impulse response samples and the other section generates the remaining samples by using interpolation. The method can be used to implement most practical FIR filters with significant savings in the number of arithmetic operations. Typically 1/2 to 1/8 of the number of multipliers and adders of conventional FIR filters are required in the implementation. The saving is achieved both in the linear phase and the nonlinear phase cases. In addition, the new implementation gives smaller coefficient sensitivities and better roundoff noise properties than conventional implementations.**

I. INTRODUCTION

FINITE impulse response (FIR) digital filters are known to have some very desirable properties like guaranteed stability, absence of limit cycles, and linear phase, if desired. The major drawback is the large number of arithmetic operations needed in the implementation. The number of multipliers in the direct form implementation is the same as the length of the impulse response sequence. In the linear phase case the number of multipliers can be reduced by approximately 50 percent. In both cases the number of adders is approximately the same as the impulse response length. However, practical FIR filters have an impulse response with a smooth predictable envelope and do not need the generality provided by standard FIR filter implementations. One can remove quite a few impulse response samples and easily find their values again with good accuracy using some type of interpolation scheme.

In this paper we describe a novel method for FIR filter design, in which this redundancy in filter coefficients has been exploited resulting in significant savings in the number of arithmetic operations. The basic idea is to implement the filter as a cascade of two FIR sections, where one section generates the sparse set of impulse response values with every Lth sample being nonzero, and the other section performs the interpolation. The interpolator can be often implemented with only a few simple arithmetic operations. The overall implementation, to be called the *interpolated finite impulse response* (IFIR) filter, typically requires approximately $1/L$th of the multipliers and adders of a conventional equivalent FIR filter. This saving can be achieved in both the linear and nonlinear phase cases. However, in this paper we concentrate on the design and analysis of linear phase IFIR filters. The reduction of multipliers also results in reduced coefficient sensitivities and roundoff noise levels as well. The number of delays is approximately the same as in the corresponding conventional implementation. The effect of interpolating the impulse response can be analyzed easily in the frequency domain. This makes it possible to develop a simple design procedure that only requires the use of a standard FIR filter design program.

There are several other methods that utilize the redundancy of the tap coefficients to achieve computationally effective FIR realizations. Thinning of the impulse response by removing some of the tap coefficients has been proposed by Smith and Farden [1]. The method gives some improvement, but the design of the filters is complicated and the resulting filter is irregular in structure because of nonuniform tap spacing. The approach proposed by Boudreaux and Parks [2] uses a low-order IIR section in cascade with uniformly or nonuniformly thinned numerator. Dynamic programming is used to optimize the performance of the cascade. The basic principle in this approach is somewhat similar with our method, the difference being that Boudreaux and Parks use the IIR section to perform the interpolation. Due to pole-zero cancellation, the overall filter has a finite length impulse response. However, the presence of feedbacks implies that the structure can have limit cycle and overflow oscillations. The method gives good results on filters with sharp cutoffs. A major difference between thinned filters and IFIR filters is in the filter design process. Our method is based on the frequency domain properties of digital interpolation as opposed to the direct optimization approach of the former.

Another approach to reduce the computational workload is via multirate filtering [3], [4], where the internal data rate is altered by using decimation and interpolation. Redundancy in the tap gains is reduced by making the actual frequency shaping at a low rate and thus with a filter with a relatively wide passband. Multirate filtering is effective in narrow-band and wide-band applications. The overall structure is, however, more complex than an IFIR filter. As the internal data rate in IFIR filters is constant there is no danger of internal aliasing, which is one of the major design considerations in multirate filtering.

In a recent paper [5] Adams and Willson describe an FIR structure composed of a recursive running sum prefilter followed by an FIR amplitude equalizer. The prefilter produces several zeros on the unit circle without any multiplications. The amplitude equalizer is used to make the overall filter meet the passband and stopband specifications. The method is

Manuscript received October 25, 1982; revised July 19, 1983. This work was supported in part by the National Science Foundation under grants ENG 79-18028 and ECS 82-18310, and in part by a University of California MICRO research grant with matching support from Intel Corporation and Rockwell International.

Y. Neuvo is with the Department of Electrical Engineering, Tampere University of Technology, Tampere, Finland.

C.-Y. Dong is with the Department of Radio-Electronics, Beijing University, Beijing, People's Republic of China.

S. K. Mitra is with the Department of Electrical and Computer Engineering, University of California, Santa Barbara, CA 93106.

0096-3518/84/0600-0563$01.00

applicable to low-pass and high-pass filters with narrow passbands. A moderate saving in the number of adders and multipliers is achieved over conventional FIR filters at the expense of a small increase in the number of delays.

II. Interpolated Impulse Response Filters

Let us consider a digital filter $H_M(z)$ with impulse response $h_M(n)$. We call this the *model filter* as it will determine the frequency behavior of the final interpolated impulse response filter.

If we insert $L - 1$ zero-valued samples between the original samples of $h_M(n)$, we obtain the sequence $h'_M(n)$

$$h'_M(n) = \begin{cases} h_M(n/L) & n = iL, i = 0, \pm 1, \pm 2, \cdots \\ 0 & \text{otherwise.} \end{cases} \tag{1}$$

The z transform $h'_M(n)$ of (1) is

$$H'_M(z) = H_M(z^L). \tag{2}$$

Thus, the implementation of $H'_M(z)$ is simply obtained from the implementation of $H_M(z)$ by replacing each delay with L delays. To generate the interpolated impulse response we cascade $H_M(z^L)$ with an interpolator $G(z)$ as shown in Fig. 1. The overall frequency response $H_i(z)$ is thus

$$H_i(z) = H_M(z^L)\, G(z). \tag{3}$$

The design of $G(z)$ is most conveniently performed in the frequency domain. Note that the frequency response of $H'_M(e^{j\omega})$ is periodic with a period of $2\pi/L$. Any of the passbands in the interval $[0, \pi]$ can be selected to be the desired one. The purpose of the interpolator is thus to attenuate the unwanted replicas of the desired passband below the prescribed level δ_2 of the overall filter. Time and frequency domain behavior of the different signals in the various stages of implementation are illustrated in Fig. 2. It is important to note that in the interpolated impulse response filter, the passband and transition bandwidths are $1/L$th of the corresponding widths of the model filter.

Let us assume that we want the gain of $H_i(z)$ of (3) to approximate 1 in the passband with a maximum deviation of δ_1 and zero in the stopband with maximum deviation of δ_2. The requirements of the overall filter are thus

$$1 - \delta_1 \leq \left|H_M(e^{jL\omega})G(e^{j\omega})\right| \leq 1 + \delta_1 \quad \text{in the passband} \tag{4a}$$

$$\left|H_M(e^{jL\omega})G(e^{j\omega})\right| \leq \delta_2 \quad \text{in the stopband.} \tag{4b}$$

Our main interest is in those cases where $H_M(e^{jL\omega})$ to a great extent determines the passband and the transition band behaviors. In addition, we assume that the passbands of $H_M(e^{jL\omega})$ are reasonably well separated. The magnitude of $G(e^{j\omega})$ should have only a slight effect on the passband shape, which if necessary can be compensated by predistorting the specifications for $H_M(z)$. We also require $H_M(z)$ to provide the stopband attenuation (4b). This makes the requirements for $G(z)$ very mild. $G(z)$ has just to provide the attenuation of the unwanted replicas of the desired passband.

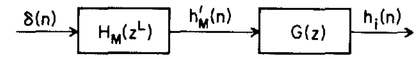

Fig. 1. Interpolated finite impulse reponse filter.

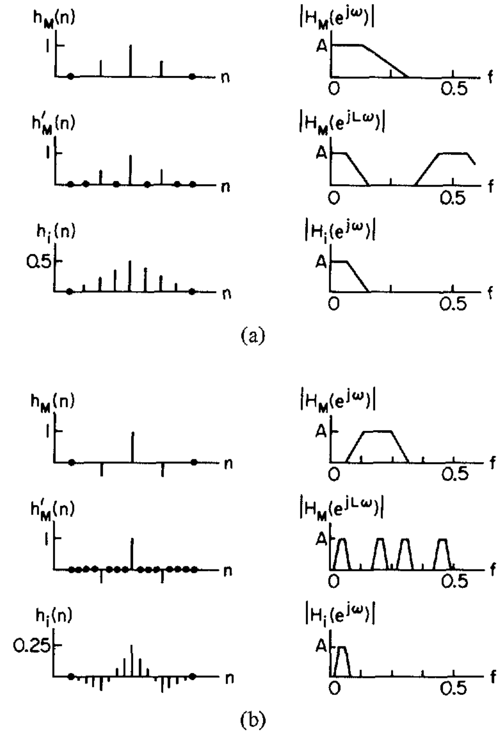

Fig. 2. Schematic forms of the signals in IFIR filters. (a) Low-pass, $L = 2$. (b) Bandpass, $L = 5$.

III. Design Procedure

Selection of L

The largest value for L, L_{MAX}, that can be used depends on the specifications of the IFIR filter. We actually want the model filter to meet the passband and stopband attenuation requirements. If the stopband edge frequency of the low-pass IFIR filter is denoted by ω_{SL}, the maximum value for L is

$$L_{\text{MAX}} = \left\lfloor \frac{\pi}{\omega_{SL}} \right\rfloor \tag{5}$$

where the brackets denote truncation. Equation (5) ensures that the model filter stopband edge is less than π. For highpass filters, we replace ω_{SL} by $\pi - \omega_{SH}$, where ω_{SH} is the stopband edge frequency of the highpass filter. The above equation can also be used for bandpass filters if the passband is centered around π/k, where k is a positive integer. In this case ω_{SL} is replaced by $(\omega_{S1} - \omega_{S2})/2$, where ω_{S1} and ω_{S2} are the desired stopband edge frequencies. For general bandpass cases L_{MAX} is the largest L that makes ω_{S1} and ω_{S2} fit into the same division of π/L.

In practice it is recommended that a somewhat smaller value than L_{MAX} be selected as the requirements for the interpolator become otherwise more stringent if it has to select one of two very close passbands of $H_M(z^L)$.

Interpolator Structures

The design of the interpolator $G(z)$ can now be formulated as the design of a multistopband FIR filter having passband matching the wanted passband of $H_M(z^L)$ and stopbands overlapping the unwanted replicas of the passband. The McClellan-Parks algorithm [6] can be used to solve this design problem However, a simpler method of choosing a low-order FIR section with one or more zeros at the desired stopbands often gives quite good results. This method also provides a saving in the number of arithmetic operations needed to implement $G(z)$ if L can be factored out into a product of small integers. In this case we can effectively utilize the periodic nature of the frequency response of digital filters to generate several stopbands at right positions.

Let the passband of the overall filter $H_i(z)$ be centered at ω_0. For $L = 2$, $H_M(z^L)$ has passbands centered at ω_0 and $\pi - \omega_0$, where we have assumed that $\omega_0 < \pi/2$. The simplest possible form of $G(z)$ for low-pass implementation is given by

$$G_0(z) = \tfrac{1}{2}(1 + z^{-1}) \tag{6}$$

which has a zero at $z = -1$. With this interpolator, the impulse response of the composite structure is

$$h_i(n) = \tfrac{1}{2}\,[h_M'(n) + h_M'(n-1)]. \tag{7}$$

Hence, this is the zero-order interpolator with $L = 2$. For high-pass cases, one can use

$$G_1(z) = \tfrac{1}{2}(1 - z^{-1}). \tag{8}$$

For bandpass cases, as well as for better performance in low-pass and high-pass cases, a second-order FIR interpolator

$$G_2(z) = \frac{1}{K}(1 + 2\cos\omega_0 z^{-1} + z^{-2}) \tag{9}$$

can be used. $G_2(z)$ has a zero pair on the unit circle at $\pi \pm \omega_0$. Here

$$h_i(n) = \frac{1}{K}\,[h_M'(n) + 2\cos\omega_0\, h_M'(n-1) + h_M'(n-2)]. \tag{10}$$

Note that ω_0 is the center frequency of the desired passband. If $\omega_0 = 0$ and $K = 4$ we get the linear interpolator as can be seen from (10). The realization of $H_i(z)$ as shown in Fig. 2(a) is for linear interpolation.

For $L = 3$, the passbands of $H_M(z^3)$ are centered at ω_0 and $(2\pi/3) \pm \omega_0$ where ω_0 is the passband in the interval $[0, \pi/3]$. For low-pass, high-pass, and bandpass cases with $\omega_0 = \pi/3$ or $2\pi/3$, the interpolator of (9) can be used. For more general bandpass cases, one can use two sections of (9) in cascade to attenuate the two unwanted passbands. If the desired passband has a center frequency close to $\pi/2$, the use of $L = 2$ can be difficult or impossible as the two passbands of $H_M(z^2)$ are close to each other and may in fact overlap. In this case the use of $L = 3$ provides good separation as the center frequencies will be approximately at $\pi/6$, $\pi/2$, and $5\pi/6$. Correspondingly there can be problems implementing bandpass filters with center frequencies close to $\pi/3$ or $2\pi/3$ if $L = 3$. Then either $L = 2$ or $L = 4$ should be used.

In the case of a very narrow passband the design may call for a large value of L. In this case it is recommended that L be selected as composite number and then build the interpolator in steps. Thus, for $L = 4$, the use of two cascaded sections with $L = 2$ is preferred. For the first section the use of

$$G_3(z) = \frac{1}{K}(1 + 2\cos 2\omega_0 z^{-2} + z^{-4}) \tag{11}$$

produces one zero on two of the undesired passbands assuming that the desired passband is centered at ω_0. The third unwanted passband can be attenuated by using $G_2(z)$. In the low-pass case, $G_3(z)$ of (11) interpolates linearly the center value and $G_2(z)$ of (9) generates the first and third value for the impulse response of $H_M(z^4)$ having three zero-valued samples between the samples of $H_M(z)$. Extension of the method to larger values of L is straightforward.

Design Steps

The design of IFIR filters can now be summarized as follows.

1) From the given filter stopband edge frequencies, calculate L_{MAX} and select a suitable $L < L_{MAX}$. After L has been selected, the positions of the unwanted repetitions of the passband are known.

2) Design the interpolator $G(z)$ to attenuate these repetitions of the passband to or below the stopband level.

3) Design the model filter $H_M(z)$. The band edge frequencies of the model filter are obtained by multiplying the edge frequencies of $H_M(z^L)$ in the interval $[0, (\pi/L)]$ by L. The model filter amplitude specifications can now be calculated from the specifications of the IFIR filter by compensating for the effect of the interpolator $G(z)$. If the passband is sufficiently narrow, no compensation is required. The design of the model filter can be done using any FIR filter design program. We used the program of McClellan and Parks [6], which is very easy to modify for the variable passband and stopband speifications.

The above procedure is for narrowband low-pass, bandpass, and high-pass filters, To design wide-band low-pass filters as well as bandstop filters, we can first design a narrow-band IFIR filter $H_i(z)$ which is the complementary filter of the final filter $H(z)$ [7]. The realization for $H(z)$ then acquires the form

$$H(z) = z^{-(N-1)/2} - H_i(z) \tag{12}$$

where the length of the filter is odd.

IV. Computational Savings

We now compare the amount of computations required by the IFIR filter with that of an equivalent conventional FIR filter meeting the same frequency domain specifications. Two examples of the IFIR implementations are shown in Fig. 3. Assuming that the hardware needed to implement the interpolator is small, we notice that the number of multipliers and adders in the structure is approximately the same as in the model filter. In IFIR filter the passband and stopband gains are the same as in the model filter, but the passband and stopband widths are only $1/L$th of those of the model filter. Thus, the effect of the interpolation of the impulse response is to shrink the passband and transition bands without any significant increase in the number of arithmetic operations.

The length of an FIR filter required to meet given specifications is approximately [8]

$$N = \frac{-20\log_{10}\sqrt{\delta_1\delta_2} - 13}{14.6\,\Delta F} + 1 \tag{13}$$

where δ_1 and δ_2 are the passband and stopband ripples, and ΔF is the relative transition bandwidth

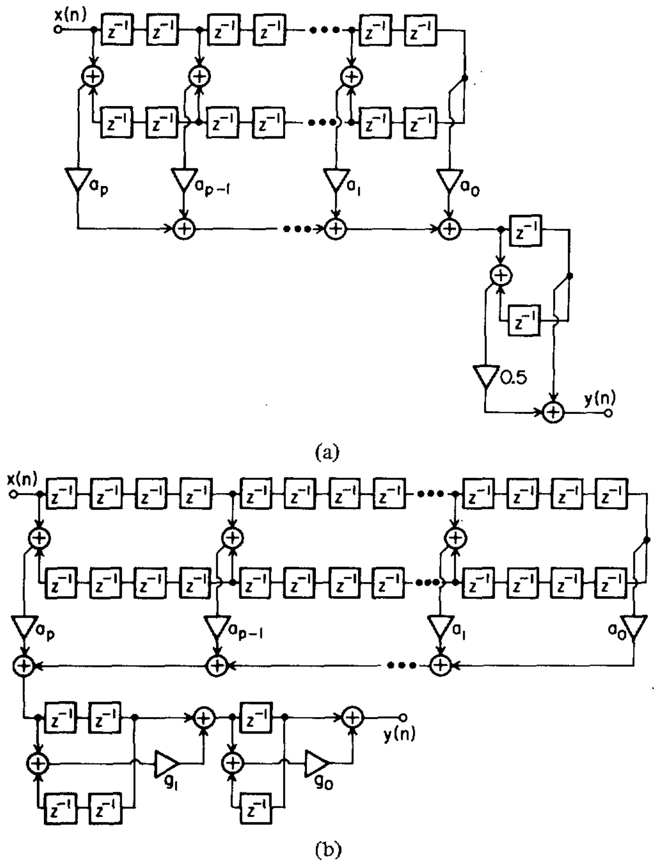

Fig. 3. IFIR filter structures. (a) Low-pass with $L = 2$. (b) Bandpass with $L = 4$ and two-stage interpolation.

$$\Delta F = \frac{\omega_s - \omega_p}{2\pi}.$$

Thus, the IFIR filter requires approximately $1/L$th of the multipliers and adders of an equivalent conventional FIR filter. In addition to neglecting the effect of the interpolator, this comparison does not take into account the oscillatory performance characteristics of optimal FIR filters. As this can slightly favor either the IFIR or the conventional FIR filter, comparison based on (13) does illustrate adequately the computational savings.

If $L = 2^J$, $J = 1, 2, \cdots$, the total number of multipliers for the type of structure shown in Fig. 3(b) is

$$M_1 = \left\lfloor \frac{N_M + 1}{2} \right\rfloor + J \tag{14}$$

where N_M is the length of the model filter. A total of J multipliers in the interpolator take a value of $\frac{1}{2}$ for low-pass filters. In the calculation of the number of the multipliers the gain constants of the interpolator subsections are merged with the tap gains of the actual filter. A comparable frequency response can be obtained with a linear phase conventional FIR filter. The number of multipliers in the conventional filter is then

$$M_C = \left\lfloor \frac{LN_M - L + 1}{2} \right\rfloor. \tag{15}$$

The number A_I of two input adders in the IFIR filter and A_C in the conventional filter are

$$A_I = N_M - 1 + 2J \tag{16}$$

$$A_C = LN_M - L. \tag{17}$$

If the number of zeros per unwanted passband is increased by a factor of P, the numbers J in (14) and (16) get multiplied by P. However, for relatively narrow-band filter specifications, N_M tends to be large and the requirements for the interpolator at the same time can be met with very few arithmetic operations. Thus, the IFIR filter requires approximately $1/L$th of the multipliers and adders of a corresponding conventional FIR filter.

The model filter and the interpolator blocks can also be merged into one block in the implementation of an IFIR filter. Fig. 4 shows this alternative structure of a low-pass IFIR filter with $L = 2$. The number of multipliers is still the same as in the structure of Fig. 3(a) but the number of adders has increased as well as the number of multipliers with coefficients. (The transpose of the structure of Fig. 4 may find use in CCD implementations, for example.)

V. Finite Wordlength Properties of IFIR Filters

Both the coefficient sensitivities and output roundoff noise properties of the IFIR filter are next analyzed and shown to be better than those of the conventional FIR filter.

An upper bound for the standard deviation of the error in the frequency response due to coefficient quantization is given by [9]

$$\sigma(\omega) \leqslant \frac{Q}{2}\left(\frac{2N-1}{3}\right) \tag{18}$$

where Q is the quantization step size and the filter length N is odd.

In the implementation of the IFIR filter, we can safely assume that the interpolator does not increase the coefficient sensitivity. This is a reasonable assumption as in the neighborhood of the passband, where the gain of the interpolator is approximately one, the distances to the zeros of the interpolator are large. Closer to the zeros of the interpolator the required stopband attenuation is exceeded so much that the coefficient sensitivity is no problem. On the unwanted replicas of the passband, the attenuation caused by the interpolator is easy to check using quantized interpolator coefficients, if necessary. Based on these arguments it is sufficient to analyze only the effect of quantizing the coefficient of $H_M(z^L)$. It is easy to see that the coefficient sensitivities of $H_M(z^L)$ will have the same upper bound for the standard deviation as the model filter $H_M(z)$ has.

If we now compare the standard deviation (σ_{CONV}) of the coefficient quantization error of a conventional filter of length LN with that of an IFIR filter (σ_{IFIR}) derived from a model filter of length N, we find, using (18), that they are related as

$$\sigma_{\text{CONV}} \approx L\sigma_{\text{IFIR}} \tag{19}$$

for large N.

The output roundoff noise variance (v_{CONV}) at the output of a conventional filter of length LN is approximately

$$v_{\text{CONV}} \approx \frac{LN}{2}\frac{Q^2}{12} \tag{20}$$

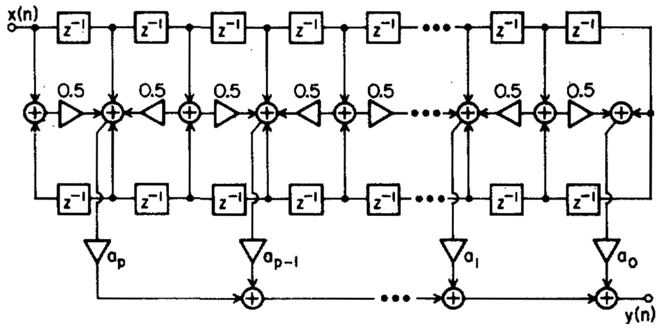

Fig. 4. Low-pass IFIR filter with $L = 2$. The linear phase interpolation is built into the structure.

if N is reasonably large. An IFIR filter derived from a model filter of length of N has the output noise variance

$$v_{\mathrm{IFIR}} = \left[\frac{N}{2}\sum_{i=0}^{M} g^2(i) + C\right]\frac{Q^2}{12} \tag{21}$$

where $g(i)$ are the impulse response coefficients of the interpolator and C comes from the noise generated in the interpolator section. If the model filter is designed to have a peak magnitude of one in the passband and the interpolator is scaled so that the maximum gain of the IFIR filter is one in the passband, it is very easy to see that the summation of $g^2(i)$ produces a number that is less than one in all practical IFIR filters. In the low-pass case, with $G_2(z)$ of (9) as the interpolator and $K = 4$, the summation over $g^2(i)$ yields 3/8. In the low-pass case with $L = 4$ the cascade of (9) and (11) yields 11/64. If the interpolator of (9) is used for the bandpass case, $K = 4 \cos \omega_0$, and the noise gain of the interpolator is less than one if $\omega_0 \leqslant 0.37\ \pi$ or $\omega_0 \geqslant 0.63\ \pi$. In the low-pass case $C = 2.5$ if a scaling multiplier of one half is in front of the interpolator and if we assume that both it and the multiplier having the value 1/2 produce the same noise as the other multipliers. In bandpass cases, as ω_0 increases from zero, C increases gradually and is 4 at $\omega_0 = \pi/3$. Similar behavior is observed if ω_0 decreases from π.

For large N and assuming that the noise gain of the interpolator is one we get

$$v_{\mathrm{CONV}} \approx L v_{\mathrm{IFIR}}. \tag{22}$$

This is often a somewhat pessimistic estimate for the IFIR filter as the noise attenuation of the interpolator more than compensates for the extra noise produced by the multipliers in the interpolator.

VI. Design Examples

We have designed several IFIR filters with varying specifications. Some illustrative examples are given next. The different steps in the design process are shown in Fig. 5. Fig. 5(a) shows for comparison an optimal linear phase low-pass reference filter with passband edge at $f_p = 0.0404$, stopband edge at $f_s = 0.0556$, and length 99. The passband and stopband have been designed with equal weights. We decided to use $L = 2$ for the IFIR filter. The model filter of length 49 is shown in Fig. 5(b). It has the same stopband attenuation as the reference filter. The shape of the passband has been predistorted to compen-

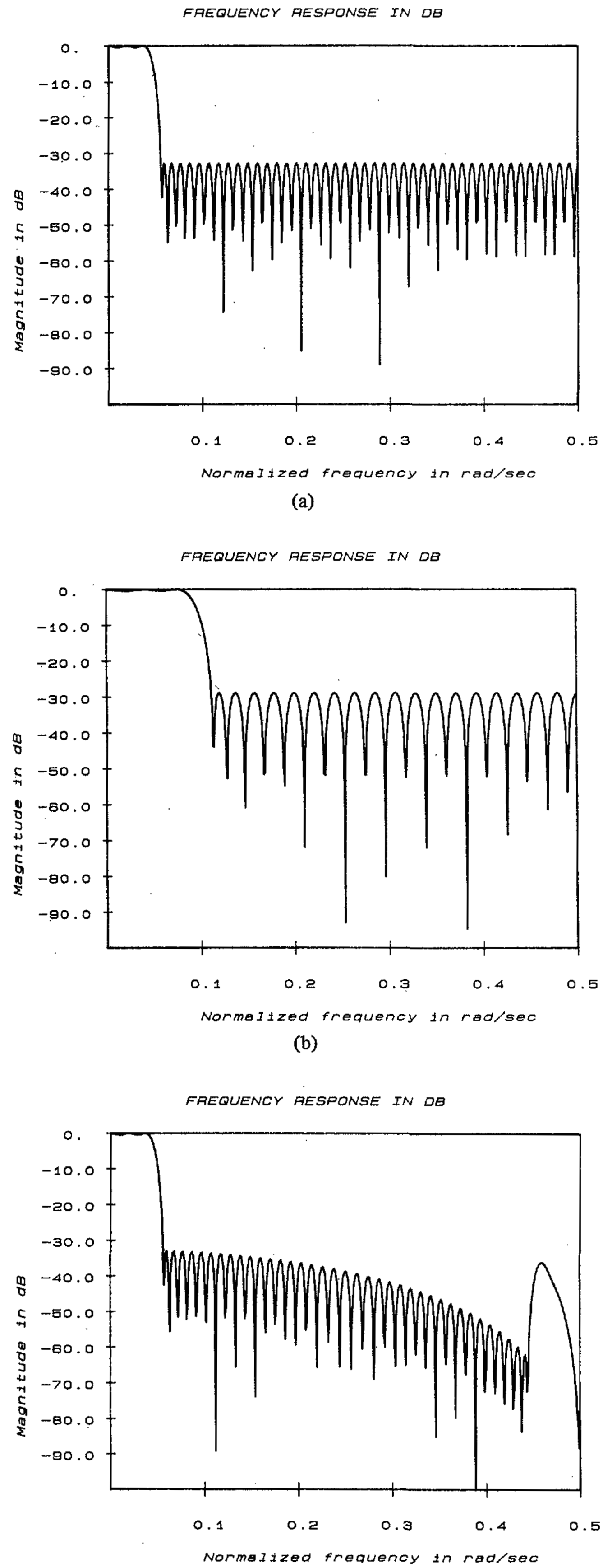

Fig. 5. Low-pass example with $L = 2$. Frequency responses of (a) reference filter of length 99, (b) model filter of length 49, (c) IFIR filter of length 99.

sate for the effect of the interpolator, although the need for compensation is questionable. It can be seen from Fig. 5(c) that the design meets essentially the same specifications as the reference filter. An IFIR filter where both the passband and stopband of the model filter have been predistorted to compensate for the effect of the interpolator is shown in Fig. 6. Comparing the response of Fig. 5(c) with that of Fig. 6(b) shows that there is no significant difference between them. The implementation for these IFIR filters is shown in Fig. 3(a). The reference filter requires 50 multiplications, 98 additions and 98 delays. The IFIR filters require 26 multipliers of which one has the value of 0.5, 50 additions, and 98 delays.

As an example of bandpass design, we considered a filter with passband edge frequencies of $f_{p1} = 0.03$, $f_{p2} = 0.05$, and stopband edge frequencies of $f_{s1} = 0.02$, $f_{s2} = 0.06$. The ripple weights are 2, 1, and 2. The optimal linear phase FIR filter of length 111 is shown in Fig. 7(a) and the corresponding IFIR filter of the same length is shown in Fig. 7(b). The IFIR filter has been designed using a model filter of length 27. The unwanted passbands have been attenuated by one zero at the center of each passband. The implementation is shown in Fig. 3(b). The number of multipliers, adders, and delays in the reference filter are 56, 110, and 110, respectively. The IFIR filter requires 18 multiplications, 30 additions, and 110 delays.

The final example is a very narrow-band low-pass filter taken from [2]. The passband edge is at $f_p = 0.001$ and the stopband edge at $f_s = 0.025$. The passband and stopband have equal weights in the design. A reference filter of length 65 is shown in Fig. 8(a) and a corresponding IFIR realization derived from a length 9 model filter using $L = 8$ is shown in Fig. 8(b). The IFIR filter exceeds the performance of the reference filter. In this case the reference filter requires 33 multipliers, 64 adders, and 64 delays. The IFIR filter has a three stage interpolator and requires eight multipliers, of which three have a value of 0.5, 14 adders, and 78 delays.

All of the design examples are summarized in Table I which also includes the results of a thinned filter design [2]. Note that the thinned filter gives a comparable result to the IFIR filter. This indicates that both methods effectively remove the redundancy from the tap coefficients.

An exact comparison with the low-pass filter of Adams and Willson [5] has not been included. They achieved aproximately $\frac{1}{3}$ reduction in the number of arithmetic operations. As their stopband edge frequency was at $\omega_s = 0.14\,\pi$, the IFIR implementation could use, for example, $L = 4$ resulting in a much more efficient implementation.

We have also implemented IFIR filters using Intel 2920 signal processor [10]. For example an IFIR filter of length 37 with $L = 2$ requires 80 instructions with seven bit coefficients. A corresponding conventional FIR filter that meets the same specifications requires 116 instructions. The IFIR filter has about half of the arithmetic operations of the FIR filter. In addition, due to smaller coefficient sensitivities, multipliers could be expressed with one bit smaller accuracy. The IFIR filter had 4 dB lower output roundoff noise level than the FIR filter.

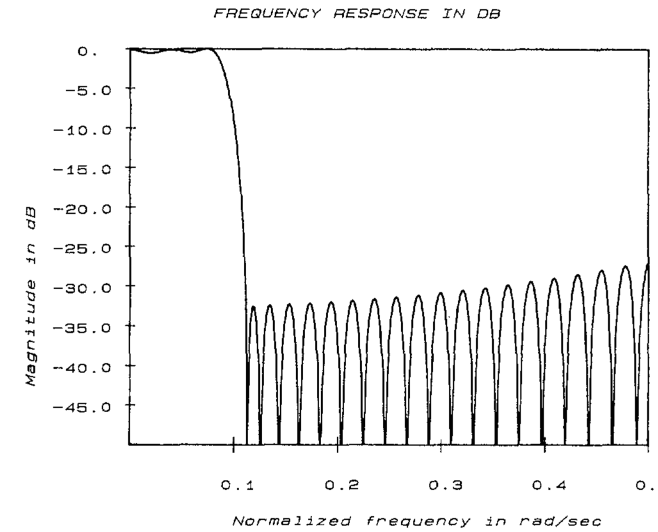

(a)

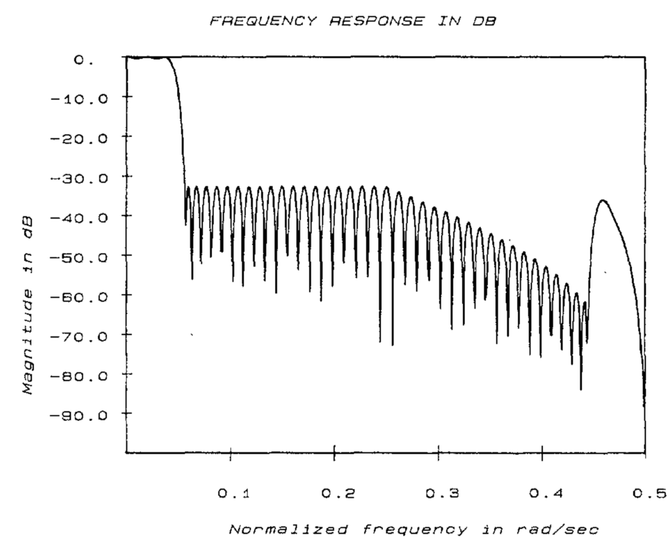

(b)

Fig. 6. IFIR filter of length 99 with both passband and stopband compensated for the attenuation of the interpolator. (a) Model filter. (b) IFIR filter.

VII. Concluding Remarks

Based on interpolation of the impulse response an efficient new method for implementing FIR filters has been derived. The IFIR filter is a cascade of a prefilter with sparse impulse response and a frequency response periodic with $2\pi/L$ (L integer) followed by an interpolator section filling the missing impulse response samples and attenuating the unwanted repetitions of the desired passband. A simple design procedure has been advanced based on a frequency domain analysis.

It has been shown that IFIR filters require approximately $1/L$th of the adders and multipliers and, in addition, have $1/L$th of the output roundoff noise level and $1/\sqrt{L}$th of the coefficient sensitivity of an equivalent conventional FIR filter.

Comparison with two recursive implementations of FIR filters indicated that IFIR filters are at least as effective in

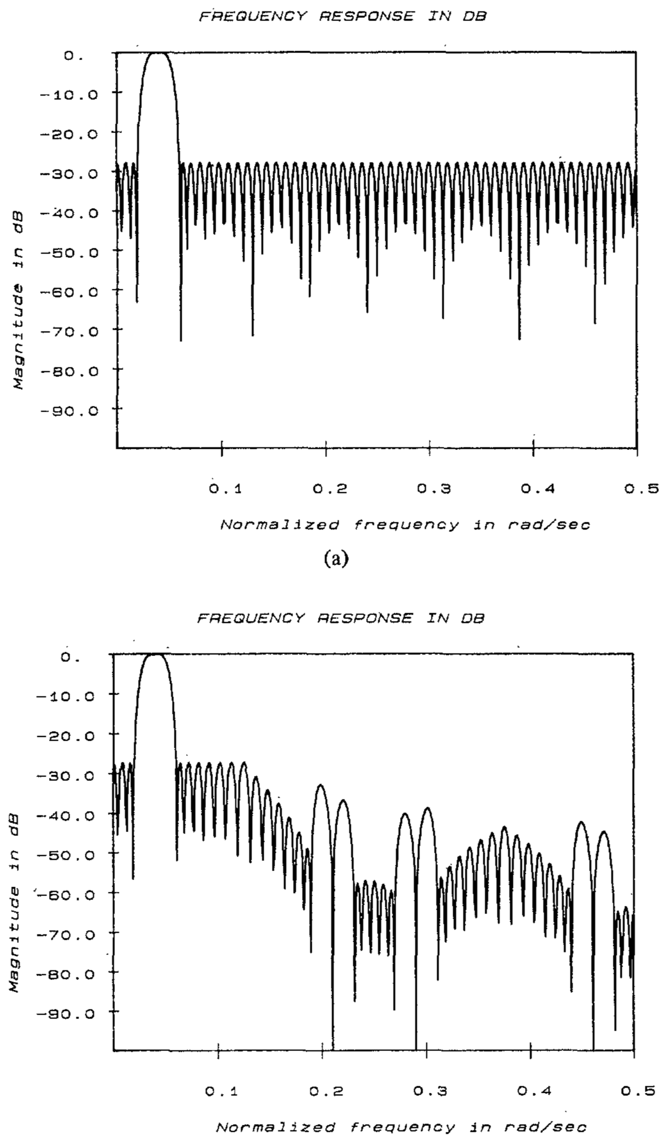

Fig. 7. Bandpass example. (a) Conventional linear phase filter of length 111. (b) Corresponding IFIR filter of the same length with $L = 4$.

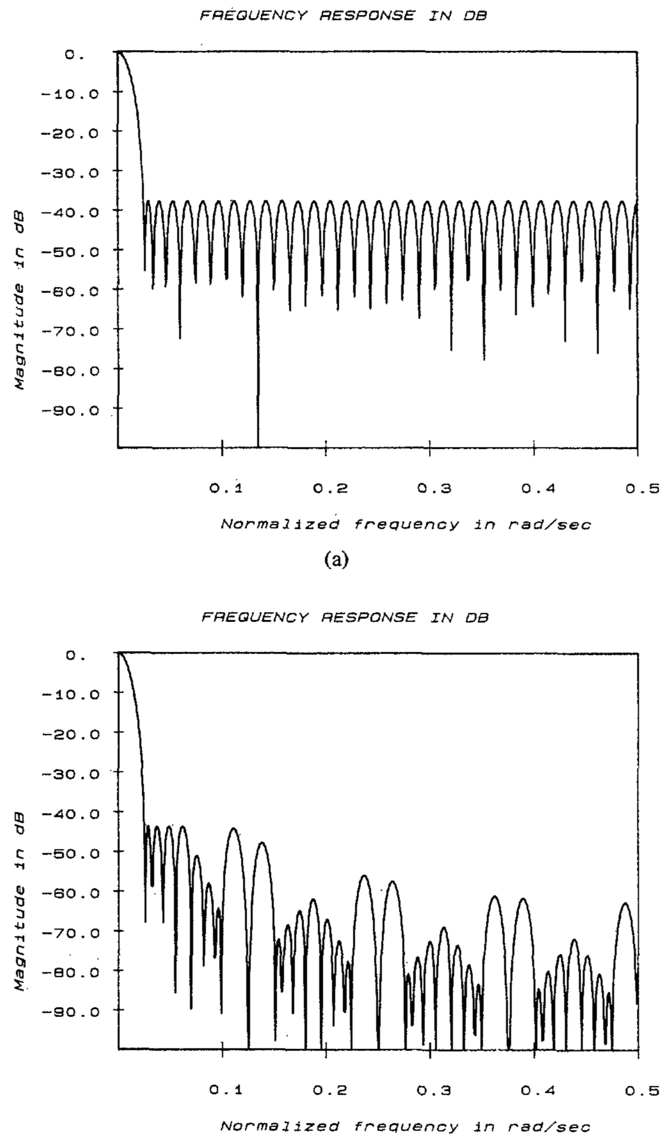

Fig. 8. Narrow-band low-pass example. (a) Conventional linear phase filter of length 65. (b) IFIR filter of length 79 derived from length 9 model with $L = 8$.

TABLE I
COMPARISON OF DESIGN EXAMPLES

Filter Specifications	Implementation	Passband Error (dB)	Stopband Error (dB)	No. of Delays	No. of Additions	No. of Multiplications[a]
low-pass	optimal FIR [Fig. 5(a)]	−0.203	−32.9	98	98	50
$f_p = 0.0404$	IFIR, $L = 2$ [Fig. 5(c)]	−0.321	−29.1	98	50	25 + (1)
$f_s = 0.0556$	IFIR, $L = 2$ [Fig. 6(b)]	−0.412	−32.7	98	50	25 + (1)
bandpass	optimal FIR [Fig. 7(a)]	−1.544	−27.8	110	110	56
$f_{p1} = 0.03, f_{p2} = 0.05$						
$f_{s1} = 0.02, f_{s2} = 0.06$	IFIR, $L = 4$ [Fig. 7(b)]	−1.646	−27.3	110	30	18
narrow-band						
low-pass	optimal FIR [Fig. 8(a)]	−0.111	−37.8	64	64	33
$f_p = 0.001$	IFIR, $L = 8$ [Fig. 8(b)]	−0.0358	−36.8	78	14	5 + (3)
$f_s = 0.025$	thinned [2]	±0.885	−34.8	NA	NA	6

[a] No. or multipliers of value 1/2 is given in parentheses.

terms of the required number of arithmetic operations and naturally eliminate the finite arithmetic problems associated with the recursive sections.

The IFIR concept can be extended to two-dimensional FIR filters with the same types of advantages as achieved in one dimension [11]. Extension to IIR filters can also be made. In IIR filters the order of a low-pass filter (Butterworth, Chebyshev, or elliptic) meeting given passband and stopband specifications is a function of the transition ratio k

$$k = \frac{\tan \frac{\omega_p}{2}}{\tan \frac{\omega_s}{2}} \tag{23}$$

where ω_p and ω_s are respectively the passband and stopband edge frequencies [12]. According to (23) we can make the filter narrower without any significant change in the number of arithmetic operations if we keep the ratio ω_p/ω_s constant. Thus, considering the number of arithmetic operations, there seems to be no major advantage obtainable in using interpolated IIR (IIIR) filters derived from conventional IIR filters. However, the use of IIIR filters may result in reducing the finite wordlength effects.

ACKNOWLEDGMENT

The simulation of filters using Intel 2920 signal processor was carried on equipment donated by Intel Corporation.

REFERENCES

[1] M. V. Smith and D. C. Farden, "Thinning the impulse response of FIR digital filters," in *Proc. 1981 IEEE Int. Conf. Acoust., Speech, Signal Processing*, Atlanta, GA, Mar. 1981, pp. 240–242.

[2] G. F. Boudreaux and T. W. Parks, "Thinning digital filters: A piecewise exponential approximation approach," *IEEE Trans. Acoust., Speech, Signal Processing*, vol. ASSP-31, pp. 105–113, Feb. 1983.

[3] M. G. Bellanger, J. L. Daquet, and G. P. Lepagnol, "Interpolation, extrapolation and reduction of computation speed in digital filters," *IEEE Trans. Acoust., Speech, Signal Processing*, vol. ASSP-22, pp. 231–235, Aug. 1974.

[4] R. E. Crochiere and L. R. Rabiner, "Optimum FIR digital filter implementations for decimation, interpolation and narrowband filtering," *IEEE Trans. Acoust., Speech, Signal Processing*, vol. ASSP-23, pp. 444–456, Oct. 1975.

[5] J. W. Adams and A. N. Willson, Jr., "A new approach to FIR digital filters with fewer multipliers and reduced sensitivity," *IEEE Trans. Circuits Syst.*, vol. CAS-30, pp. 277–283, May 1983.

[6] J. H. McClellan, T. W. Parks, and L. R. Rabiner, "A computer program for designing linear phase FIR filters," *IEEE Trans. Audio Electroacoust.*, vol. AU-21, pp. 506–526, Dec. 1973.

[7] R. M. Golden, "Digital filters," in *Modern Filter Theory and Design*, G. C. Temes and S. K. Mitra, Eds. New York: Wiley, 1973, ch. 12.

[8] J. F. Kaiser, "Nonrecursive digital filter design using the I_0-sinh window function," in *Digital Signal Processing II.* New York: IEEE Press, 1975, pp. 123–126.

[9] L. R. Rabiner and B. Gold, *Theory and Application of Digital Signal Processing.* Englewood Cliffs, NJ: Prentice-Hall, 1975, sec. 5.30, pp. 346–349.

[10] *2920 Analog Signal Processor Design Handbook*, Intel Corporation, Santa Clara, CA 1980.

[11] M. V. Thomas, Y. Neuvo, and S. K. Mitra, "Two-dimensional interpolated finite impulse response filters," in *Proc. 1983 IEEE Int. Symp. Circuits Syst.*, Newport Beach, CA, May 1983, pp. 104–106.

[12] L. R. Rabiner and B. Gold, *Theory and Application of Digital Signal Processing.* Englewood Cliffs, NJ: Prentice-Hall, 1975, sec. 4.10, pp. 238–252.

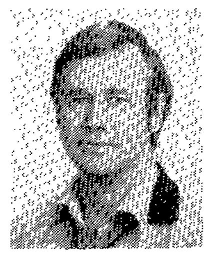

Yrjö Neuvo (S'70–M'74–SM'82) was born in Turku, Finland, on July 21, 1943. He received the Diploma Engineer and Licentiate of Technology degrees from the Helsinki University of Technology, Helsinki, Finland, in 1968 and 1971, respectively, and the Ph.D. degree in electrical engineering from Cornell University, Ithaca, NY, in 1974.

He held various research and teaching positions at the Helsinki University of Technology, the Academy of Finland, and Cornell University, from 1968 to 1976. Since 1976 he has been a Professor of electrical engineering at the Tampere University of Technology, Tampere, Finland. During the academic year 1981–1982 he was with the University of California, Santa Barbara as a Visiting Professor. His main research interests are in the areas of digital filters and microcomputer systems.

Dr. Neuvo is a member of Phi Kappa Phi and the Finnish Academy of Technical Sciences.

Dong Cheng-yu graduated in 1964 from the Department of Radio-Electronics, Beijing University, People's Republic of China.

Since 1964 he has been with the Department of Radio-Electronics, Beijing University, in teaching and research positions. His research has involved signal detection, laser, sonar, and radar systems. He was a visiting research scholar at the University of California, Santa Barbara, from 1980 to 1982. At present he is engaged in research in digital signal processing.

Mr. Dong is a member of Beijing Institution of Electronics.

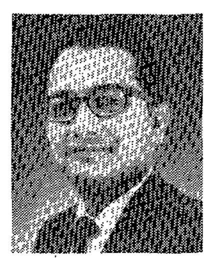

Sanjit K. Mitra (S'59–M'63–SM'69–F'74) received the B.S. (Honors) degree in physics from the Utkal University, India, in 1953, the M.Sc. (Tech.) degree in radio physics and electronics from the University of Calcutta, India, in 1956, and the M.S. and Ph.D. degrees in electrical engineering from the University of California, Berkeley, in 1960 and 1962, respectively.

He joined the faculty of the University of California, Davis in 1967 and transferred to the University of California Santa Barbara campus in 1977 as a Professor of Electrical and Computer Engineering. From July 1979 to June 1982 he served as the Chairman of the Department of Electrical and Computer Engineering at UCSB. He is a Consultant to the Lawrence Livermore National Laboratory, Livermore, CA, and has served as a consultant to the Ampex Corporation, Fairchild Semiconductors, GM Delco Electronics, Siliconix, the U.S. Army, and World Bank. He has held visiting appointments at the Indian Institute of Technology, New Delhi, India, Kobe University, Japan, the University of Erlangen-Nuernberg, West Germany, and the Australian National University, Canberra. He has published a number of papers in active and passive networks and digital filters, and is the author of two texts and editor/co-editor of three other books. He is the Consulting Editor for the *Electrical/Computer Science and Engineering Series* of the Van Nostrand Reinhold Company, NY.

Dr. Mitra is a Fellow of the American Association for the Advancement of Science and a member of the American Society for Engineering Education, Sigma Xi, and Eta Kappa Nu. He was an Associate Editor of the IEEE TRANSACTIONS ON CIRCUITS AND SYSTEMS, a member of the Administrative Committee of the IEEE Circuits and Systems Society, and a member of the editorial boards of the IEEE Press and PROCEEDINGS OF THE IEEE. He was the General Chairman of the 1974 IEEE International Symposium on Circuits and Systems, and Technical Program Chairman of the 1983 IEEE International Symposium on Circuits and Systems. He is also the recipient of the 1973 F. E. Terman Award of the American Society for Engineering Education.